第94卷 第3期 地 质 学 报 ACTA GEOLOGICA SINICA Vol. 94 No. 3
2020年3月 Mar. 2020

阿尔金断裂东段的构造转换模式

罗浩[1)]，徐锡伟[2)]，刘小利[3)]，白鸾羲[4)]，王启欣[4)]，李梦妮[4)]，刘少卓[4)]

1）中国地震灾害防御中心，北京，100029；2）中国地震局地壳应力研究所，北京，100085；

3）中国地震局地震研究所，地震大地测量重点实验室，武汉，430071；

4）中国地震局地质研究所，活动构造与火山重点实验室，北京，100029

内容提要：大型走滑断裂控制着青藏高原的变形，众多学者通过阿尔金断裂来探索青藏高原北部的构造变形过程。基于野外调查和前人的研究结果可知阿尔金断裂的滑动速率在肃北—疏勒河口段表现为三联点两侧的突降，祁连山西段的逆冲和走滑断裂吸收了阿尔金断裂的左旋位移。由于祁连山内部次级断裂活动性的增强，现存阿尔金断裂连续地表破裂终止于酒泉盆地西侧，但位于其东侧的断裂系仍属于阿尔金断裂。在Kohistan岛弧与欧亚板块碰撞之后，青藏高原沿阿尔金断裂曾发生滑动速率近一致的侧向挤出，断裂两侧此时并未发生明显的隆起。随后东昆仑造山带和祁连山造山带的先后大规模隆升，高原的北东向挤出迅速减弱。阿尔金断裂北东向挤出能力与东昆仑造山带和祁连山造山带的隆起存在明显的耦合作用。

关键词：走滑断层；变形模式；阿尔金断裂；祁连山；青藏高原

印度-欧亚板块的碰撞在青藏高原内部和边界形成数条大型走滑断裂，如海原断裂、阿尔金断裂、东昆仑断裂和鲜水河断裂等（Molnar and Tapponnier，1978；Tapponnier et al.，2001；Zhang Yongshang et al.，2016；Zhang Yueqiao et al.，2016）。在走滑断裂的端部通常发育张性伸展构造或挤压性隆起构造（Molnar and Caent，1989；Van der Woerd et al.，1998，2000；Yin et al.，1999；Xu Xiwei et al.，2005；Kirby et al.，2007；Yu Hongmei et al.，2014；Lu Haijian et al.，2016）。断层的伸展作用形成了相对平坦的高原内部，而挤压作用形成了青藏高原边界陡峭的地貌（Tapponnier et al.，2001）。其中，阿尔金断裂控制着青藏高原北部的几何特征和构造框架，是调节青藏高原的变形和物质北东向挤出的重要断裂之一（Meyer et al.，1998；Burchfiel et al.，1989；Molnar et al.，2009；Cuningham et al.，2016；Yun Long et al.，2019）。部分学者认为阿尔金断裂左旋位移为300～500 km（Cowgill，2001；Yue et al.，2001；Yin et al.，2002），在其东端左旋位移量减小，减少量转换为祁连山北西向条脊型山脉的隆升运动（Xu Xiwei et al.，2005；Luo Hao et al.，2013b，2015，2019；Zheng Wenjun et al.，2013a）（图1）。

目前阿尔金断裂东段与祁连山西段一系列断层的转换模式鲜有介绍。Xu Xiwei et al.（2005）获取的阿尔金断裂的滑动速率支持断裂在其东端非线性减小，而Zhang Ning（2016）给出的滑动速率则显示阿尔金断裂东端符合线性减小的活动方式。祁连山地区以何种方式吸收阿尔金断裂的左旋位移，是断层的脆性转换，还是连续的褶皱变形尚不清楚（Cuningham et al.，2016）。

同时关于阿尔金断裂东端点是否延伸出祁连山区域也存在争议。一种观点认为阿尔金断裂终止于玉门盆地北侧的宽滩山断裂附近（Burchfiel et al.，1989；国家地震局《阿尔金滑动断裂带》课题组，1992；Qiu Aimei and Li Baixiang，2011；Yu Jingxing et al.，2013；Zheng Wenjun et al.，

注：本文为地震科研行业专项“中国地震活断层探察—南北地震带北段”（编号20140802306）、中国科学院战略性先导科技专项（A类）课题（编号XDA20070300）和国家自然科学基金项目（编号U1839204、41372217）资助的成果。

收稿日期：2019-09-11；改回日期：2020-01-06；网络发表日期：2020-01-20；责任编辑：周健。

作者简介：罗浩，男，1980年生。博士，副研究员，主要从事地震地质和地质灾害方面的工作。Email：hy-luo@163.com。

引用本文：罗浩，徐锡伟，刘小利，白鸾羲，王启欣，李梦妮，刘少卓. 2020. 阿尔金断裂东段的构造转换模式. 地质学报，94(3)：692～706，doi：10.19762/j.cnki.dizhixuebao.2020135.

Luo Hao，Xu Xiwei，Liu Xiaoli，Bai Luanxi，Wang Qixin，Li Mengni，Liu Shaozhuo. 2020. The structural deformation pattern in the eastern segment of the Altyn Tagh fault. Acta Geologica Sinica，94(3)：692～706.

2013b；Zhang Ning，2016；Yu Jingxing et al.，2016）。阿尔金断裂的走滑分量被祁连山及玉门盆地的逆冲断裂系吸收殆尽，青藏高原的物质并未沿断裂传输到高原外侧；部分学者认为阿尔金断裂穿过金塔盆地向东延伸，进入阿拉善块体内部并继续东延（Zheng Jiandong，1991；Darby et al.，2005；Chen Wenbin and Xu Xiwei，2006；Zhang Peizhen et al.，2007），甚至通过蒙古地区进入鄂霍次克海（Yue and Liou，1999；Yue et al.，2001）。该观点认为青藏高原物质沿阿尔金断裂北东向挤出至青藏高原外侧。解释这个争议需要了解阿尔金断裂长期的活动方式，以及与其他相关构造的转换模式。

因此，我们对阿尔金断裂的东段以及祁连山西段的相关断裂和褶皱进行了野外考察，探讨了阿尔金断裂东段的构造转换模式，并结合前人相应的研究成果讨论了阿尔金断裂东端点的位置以及阿尔金断裂一种可能存在的长期演化模式。

1 地质背景

阿尔金断裂，长约 1600 km，位于青藏高原北侧，为一个岩石圈规模的大型左旋走滑断裂，是欧亚变形场的主要构造之一（Avouac and Tapponnier，1993；Wittlinger et al.，1998）。该断裂控制着青藏高原的北边界，构成了高海拔构造变形强烈的青藏高原与低海拔构造活动薄弱的塔里木盆地的界限（Peltzer et al.，1989；Tapponnier et al.，2001），可能吸收了 1/3 或者 1/6 欧亚板块的汇聚量（Avouac and Tapponnier，1993；Xu Xiwei et al.，2005；Cowgill，2007；Zhang Peizhen et al.，2007）。关于断裂左旋剪切的初始时间存在较大争议，部分研究认为自从印度-欧亚板块碰撞开始，阿尔金断裂就开始发生大规模的左旋位移（Peltzer and Tapponnier，1988；Yin et al.，2002；Darby et al.，2005）；另外的研究认为阿尔金山段自约 15 Ma 开始发生大规模的左旋位移（Wu Lei et al.，2012a，b，2013）。断裂的左旋活动已经引起肃北、大别盖-柳城子新近纪地层（约 16 Ma）发生 60～90 km 位移（Wang Erchie，1997）；约 14 Ma 以来党河南山西段，与阿尔金断裂相交处开始发生大规模的隆升（Lin Xu et al.，2015；Sun Jimin et al.，2005），说明至少 14 Ma 阿尔金断裂东段已开始发生左旋位移。Meyer et al.（1998）和 Me′tivier et al.（1998）指出断裂活动可能始于中新世。Hanson（1999）基于西柴达木盆地接收阿尔金山物质沉积的时间认为断裂至少在

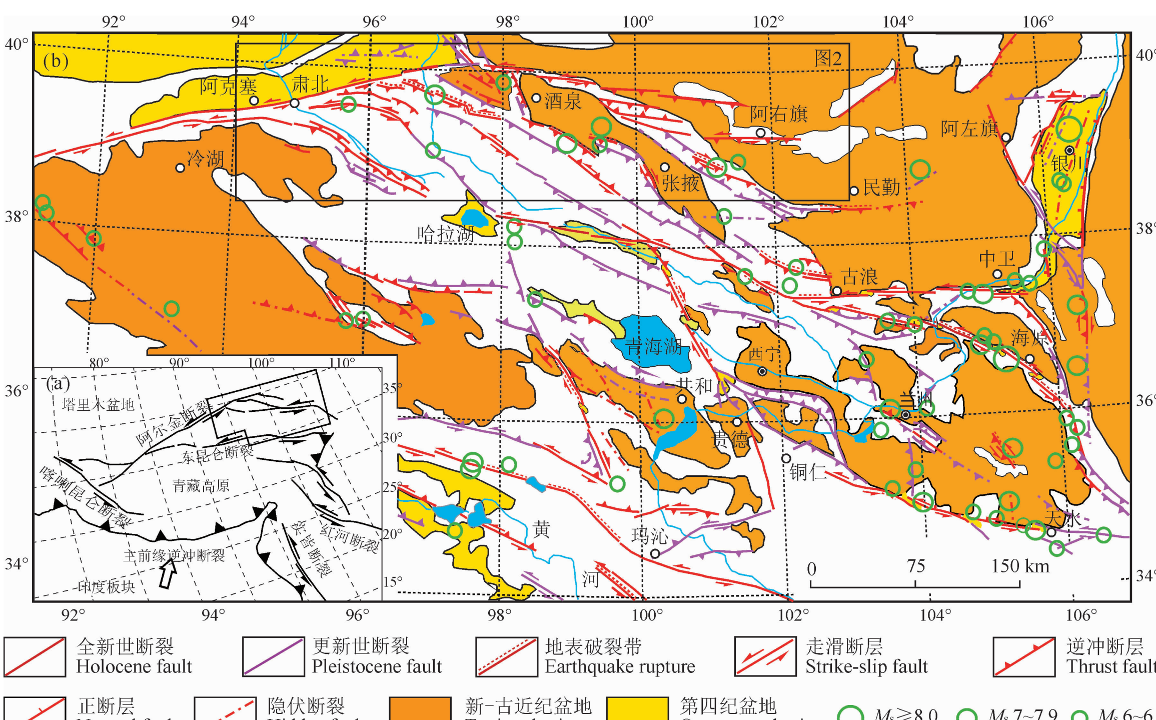

图 1 区域构造图（a）及青藏高原东北缘活动断裂展布图（b）（据 Yuan et al.，2011 修改）

Fig. 1 Regional plate tectonic setting (a) and spatial distribution of active faults in northeastern margin of Qinghai-Tibetan Plateau (after Yuan et al.，2011)

渐新世已经形成。还有一些学者认为阿尔金断裂在晚三叠纪就开始活动(Li Haibing et al. 2000)。而 Delville et al.(2001)则指出阿尔金断裂的左旋剪切活动在 160 和 140 Ma 就得以发展。

阿尔金断裂第四纪滑动速率研究很多,但并未得到很好的一致性。基于断错的地貌特征和断层地貌相应地貌面的测年,部分研究结果认为自中新世以来青藏高原沿阿尔金断裂发生大规模的左旋位移,阿尔金断裂全新世平均滑动速率为 20～30 mm/a(Me′riaux et al., 2004; Xu Xiwei et al., 2005),中国中西部地区的新构造变形均与其左旋走滑运动有关。另一方面,部分学者认为阿尔金断裂的左旋滑动速率在 10 mm/a 左右(Cowgill et al., 2007, 2009; Zhang Peizhen et al., 2007; Gold et al., 2009, 2011),例如最近 GPS 调查给出的滑动速率是 10±2 mm/a(Bendick et al., 2000; Wallace et al., 2004; He Jiankun et al. 2013)。但是二者一致认为在断裂的东段滑动速率明显减小(Meyer et al., 1996; Xu Xiwei et al., 2005; Zhang Peizhen et al., 2007; Seong et al., 2011)。

阿尔金断裂段的地震活动和滑动速率与其他段落存在明显的差异。Xu et al.(2005)认为在肃北县、石包城以及疏勒河,阿尔金断裂分别与党河南山断裂、鹰嘴山断裂和祁连山北缘断裂斜交,形成构造转换的三联点。阿尔金断裂东段的左旋位移的减小量部分通过三联点转换为这些逆断层的地壳缩短和上盘推覆体的隆起作用,形成了党河南山、大雪山和祁连山等北西向山地(图 1)。部分左旋位移通过祁连山内部的左旋走滑断层分段转换为海原断裂的左旋走滑活动(Tapponnier et al., 2001; Luo Hao et al., 2015)。

2 阿尔金断裂与祁连山的构造转换模式

2.1 肃北转换区活动断裂发育特征

在肃北县西南,阿尔金断裂与党河南山断裂西段相交(Van der Woerd et al., 2001; Shao Yanxiu et al., 2011)。党河南山断裂及其相关断裂表现为两种运动模式,断裂的逆冲活动和水平走滑活动(图 2)。在别盖乡西党河南山断裂西段分解为三条断裂,党河南山断裂东段,以逆冲变形为主,野马河南缘断裂,以走滑变形为主,以及野马河-大雪山断裂,以走滑变形为主。

党河南山断裂西段表现为数排的近似平行的断层(Van der Woerd et al., 2001),根据现场调查至少可以确定北侧的 2～3 排次级断裂为全新世活动

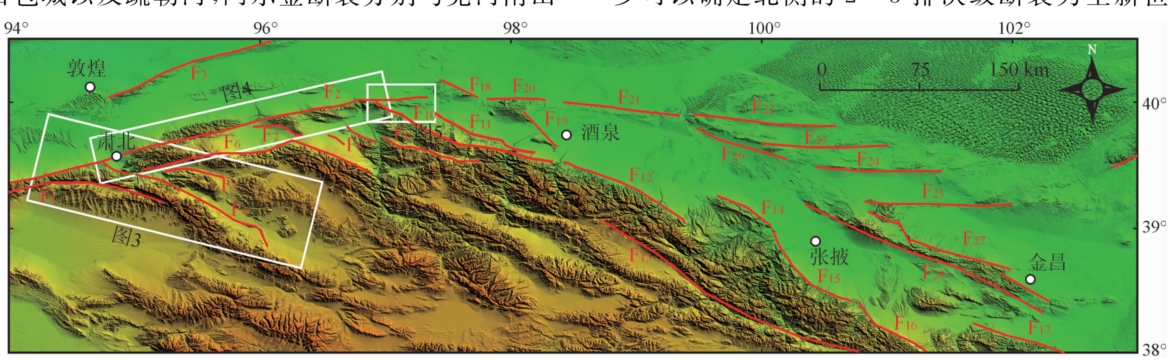

图 2 祁连山西段活动断裂展布图

Fig. 2 Spatial distribution of active faults in west segment of Qilian Mountain

F$_1$—阿尔金南缘断裂;F$_2$—阿尔金北缘断裂;F$_3$—三危山断裂;F$_4$—党河南山断裂;F$_5$—野马河南缘断裂;F$_6$—野马河-大雪山断裂;F$_7$—鹰嘴山南缘断裂;F$_8$—北山断裂;F$_9$—昌马断裂;F$_{10}$—旱峡-大黄沟断裂;F$_{11}$—玉门断裂;F$_{12}$—佛洞庙-红崖子断裂;F$_{13}$—肃南断裂;F$_{14}$—榆木山北缘断裂;F$_{15}$—榆木山东缘断裂;F$_{16}$—扁都口-军马场断裂;F$_{17}$—莲花山北缘断裂;F$_{18}$—登登山断裂;F$_{19}$—嘉峪关断裂;F$_{20}$—黑山断裂;F$_{21}$—金塔南山断裂,F$_{22}$—慕少梁南缘断裂,F$_{23}$—盘头山-羊圈沟断裂;F$_{24}$—天城-苏亥阿木断裂;F$_{25}$—阿右旗断裂;F$_{26}$—合黎山断裂;F$_{27}$—龙首山北缘断裂;F$_{28}$—龙首山南缘断裂带

F$_1$—South Altyn Tagh fault; F$_2$—North Altyn Tagh fault; F$_3$—Sanweishan fault; F$_4$—Danghe South Mountain fault; F$_5$—Yema River South fault; F$_6$—Yema River-Daxue Mountain fault; F$_7$—South margin of Yingzui Mountain fault; F$_8$—North Mountain fault; F$_9$—Changma fault; F$_{10}$—Hamxia-Dahuanggou fault; F$_{11}$—Yumen fault; F$_{12}$—Fodongmiao-Hongyazi fault; F$_{13}$—Sunan fault; F$_{14}$—Nourth margin of Yumu Mountain fault; F$_{15}$—East margin of Yumu Mountain fault; F$_{16}$—Biandukou-Junmachang fault; F$_{17}$—North margin of Lianhua Mountain fault; F$_{18}$—Dengdeng Mountain fault; F$_{19}$—Jiayuguan fault; F$_{20}$—Hei Mountain fault; F$_{21}$—Jinta South Mountain fault; F$_{22}$—South margin of Mushaoliang Mountain fault; F$_{23}$—Pantou Mountain-Yangjian Gulley fault; F$_{24}$—Tiancheng-Suhaiamu fault; F$_{25}$—Ayouqi fault; F$_{26}$—Heli Mountain fault; F$_{27}$—North margin of Longshou Mountain fault; F$_{28}$—South margin of Longshou Mountain fault

断裂。它们断错了 N_1 地层顶部黄土沉积，该地区的黄土沉积通常小于 15 ka（Meyer et al.，1998；Chen et al.，2013）。前缘断层逆冲至最新的河流阶地之上，T_1 阶地形成于 4.5 ka 左右，T_3 则形成于 13 ka（Van der Woerd et al.，2001）。与阿尔金断裂相交处，党河南山断裂最新活动表现为 2 排近平行的陡坎，与阿尔金断裂斜交，角度约为 30°。两排相距约 70 m，南侧陡坎高度约 100 cm，北侧陡坎高度约为 20 cm，未见明显的左旋滑动（图 3a）。在其东南方向断裂则表现为 T_1 高约 3 m 正向陡坎，T_2 阶地表现为高约 20 m 的正向陡坎，T_3 阶地以上的陡坎高度大于 30 m（Van der Woerd et al.，2001）（图 2b）。山前最新一级洪积扇上发育两排正向陡坎，陡坎高度 1.5～2 m，均为见到水平活动。洪积扇上最新冲沟发育两级阶地，T_1 陡坎高度为 0.5 m 表面该组断裂曾发生 2 次以上的活动（图 3c）。这说明党

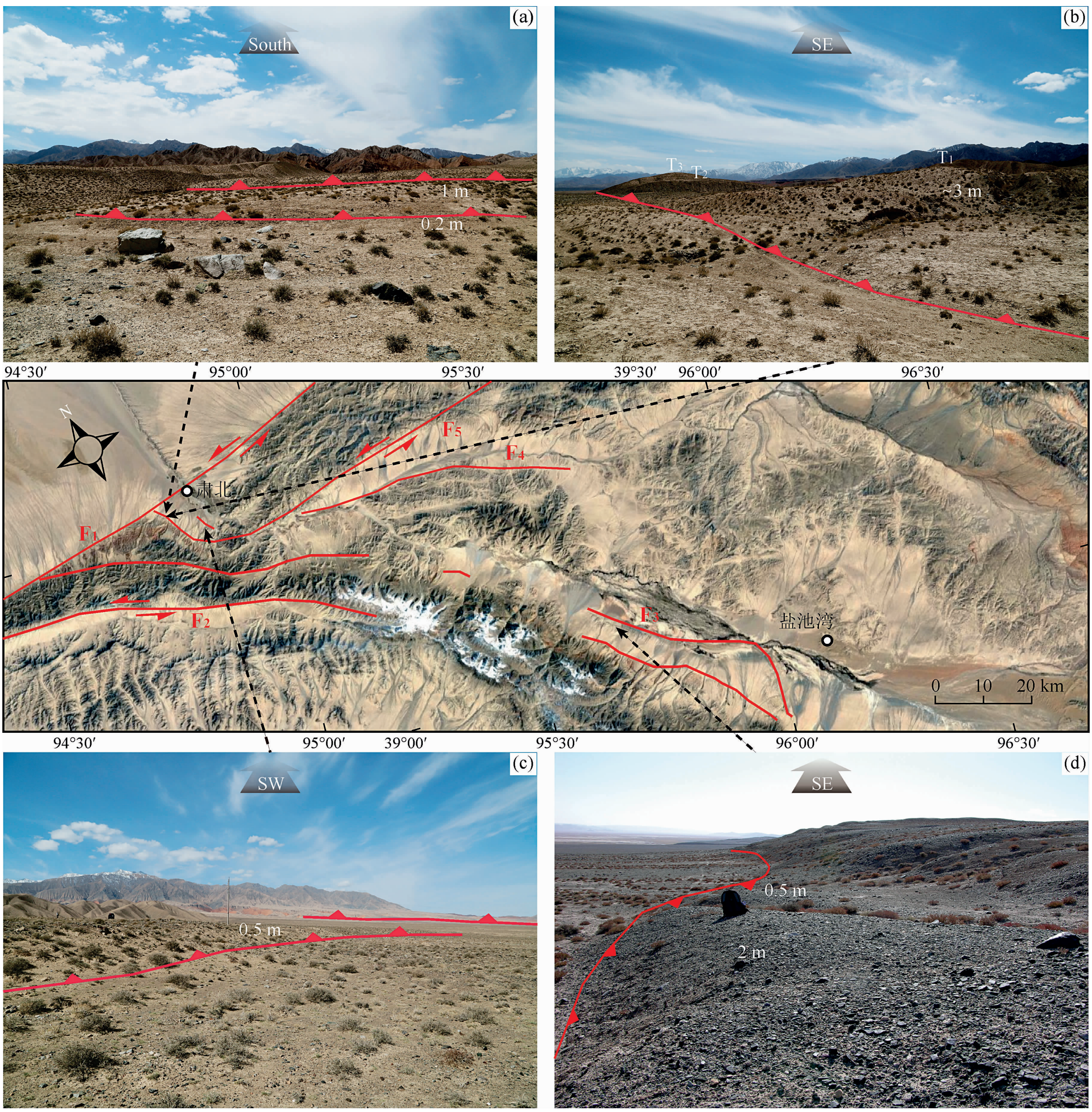

图 3　党河南山断裂构造地貌特征

Fig. 3　Structural geomorphic characteristics of the Danghe South Mountain fault

(a)—党河南山西端两排断层陡坎；(b)—党河南山西段断层陡坎；(c)—党河南山西段最新地表破裂；(d)—党河南山东段断层陡坎；F_1—阿尔北缘金断裂；F_2—阿尔金南缘断裂；F_3—党河南山断裂；F_4—野马河南缘断裂；F_5—野马河-大雪山断裂

(a)—Two fault scarps in west end of the Danghe South Mountain fault; (b)—fault scarp in west segment of the Danghe South Mountain fault; (c)—rupture in west segment of the Danghe South Mountain fault; (d)—fault scarp in east segment of the Danghe South Mountain fault; F_1—South Altyn Tagh fault; F_2—North Altyn Tagh fault; F_3—Danghe South Mountain fault; F_4—Yema River South fault; F_5—Yema River-Daxue Mountain fault

河南山断裂西段主要以叠瓦状逆冲活动为主，并向北东方向扩展。

党河南山断裂东段主要表现为逆冲变形(图3d)，在盐池湾段以两排全新世活动的陡坎展示。其东北侧形成盐池湾褶皱，枢纽北东向倾伏，北东侧表现为逆冲活动，漫滩上形成高约 50 cm 北向陡坎，表明该点最近发生过明显的构造活动。盐池湾背斜主要有 N_1、N_2 及 Q_1 地层组成，N_1、N_2 为整合接触，并且 N_2 地层表现为明显的同构造生长性质，说明该期间该地区已经开始隆起变形，N_2 与 Q_1 间为角度不整合。

野马河南缘断裂主要表现为左旋滑动，参考 Zheng Wenjun et al. (2013a)的研究结果，其滑动速率更接近 1.9±0.4 mm/a。野马河-大雪山断裂中西段以左旋为主，基于与区域应力的夹角表现为挤压或者拉张性质，滑动速率为 2.81±0.32 mm/a (Luo Hao et al., 2015)。而东段则以逆冲变形为主，山前洪积扇上普遍分布高约 8～10 m 的正向陡坎，部分残余老洪积扇前陡坎高度可达约 30 m，最新洪积扇或者阶地上的陡坎高度在 1 m 左右。探槽揭示的断层倾角在 30°～40°之间(Luo Hao et al., 2013b)，但是局部的冲沟，或者小型洪积扇中脊均发生了左旋的活动。因此我们认为由于断层的走向变化，野马河-大雪山断裂的活动性质则表现出明显的差异。断裂的中西段与阿尔金断裂东段近似平行，断裂表现出高角度(60°～90°)走滑活动为主。野马河-大雪山断裂东段与阿尔金断裂东段大角度斜交，因此断裂的活动以低角度逆冲变形为主，但仍具有左旋走滑的性质，野马河-大雪山断裂的上盘可能发生顺时针旋转的活动。

总之，在肃北三联点，阿尔金断裂东段的走滑分量部分被党河南山断裂西段所吸收，吸收量为 4±2 mm/a(Van der Woerd et al., 2001)，在别盖乡以东转化为党河南山断裂东段的逆冲活动；野马河南缘断裂和野马河-大雪山断裂的走滑活动。在肃北三联点—石包城三联点间阿尔金断裂并未发现明显的分支断层以及褶皱变形。在石包城三联点附近踏实山中发育数条的线性特征，但未见新活动，或者全新世活动很弱，无法大规模分解阿尔金断裂的左旋活动。且在肃北县城北侧，Xu Xiwei et al. (2005)和 Zhang Peizhen et al. (2007)得到的滑动速率明显低于三联点以西的速率。可认为阿尔金断裂在通过党河南山断裂西段时，近一半的缩短速率被一系列逆断层及上盘的断层相关褶皱所吸收。因此该段滑动速率的减小模式为滑动速率突变，非线性减小。

2.2 石包城转换区活动断裂发育特征

鹰嘴山南缘断裂在石包城西侧与阿尔金断裂斜交，向东沿鹰嘴山南缘展布，长约 50 km，总体呈北西西-东西向展布(图 2)。鹰嘴山南缘断裂根据其走向可分为两个次级段落。其中西段表现为明显的逆冲陡坎，由北向南逆冲，不同的河流阶地被断错 1.5～15 m(图 4a,b)。最新的冲沟活动同时展现出水平的滑动(图 4c,d)，水平的位移略大于垂直位移。在断裂的东段，主要表现为断层的垂向变形，形成平缓的正向陡坎，局部仍可见到左旋的位移，说明在该断裂的东段仍具有一定的左旋滑动分量。与野马河-大雪山断裂类似，鹰嘴山南缘断裂的下盘沿断裂具有顺时针旋转的趋势。

作为该区域的主要转换断层之一的昌马断裂各段具有不同的左旋滑动速率，西段为 1.33±0.39 mm/a、中西段 3.11±0.31mm/a、中东段 3.68±0.41 mm/a，由西向东左旋滑动速率具有递增现象，西段的缩短速率 0.70±0.20 mm/a(Luo Hao et al., 2013a)。昌马断裂的活动主要来源继承鹰嘴山南缘断裂的变形。然而鹰嘴山南缘断裂活动性明显弱于昌马断裂西段，似乎可能继承其他断层的位移。

在巴个峡地区，影像上显示出一段地貌线性良好，具有最全新世活动的可能性。而且该段断层有可能与昌马断裂处于同一个断层系统，野外考察表明该段断层地貌并未发现全新世活动，或者说晚更新世以来活动性很弱。而且在石盆湾两侧所获取的水平滑动速率保持一致(Meyer et al., 1996; Xu Xiwei et al., 2005; Seong et al., 2011; Li Yuhang et al., 2015)，可认为该段线性地貌并未明显转换阿尔金断裂的左旋滑动量。

Meyer et al. (1998)指出 1932 年昌马地震同时引起北山断裂发生破裂，可以推测昌马断裂与北山断裂和野马河-大雪山断裂在深部汇入统一滑脱面，我们认为大野马河-大雪山断裂中西段的走滑位移可以部分地转换为昌马断裂西段的逆冲和走滑的活动。东向昌马断裂水平滑动速率的增加也可能来自于野马河-大雪山的走滑活动转换。

石包城构造转换区与肃北转换区近似，在石包城—疏勒河口段左旋滑动速率近似一致，构造转换区两侧的滑动速率表现为突然减小。作为石包城转换区的主要构造，昌马断裂可能部分承担了肃北构造转换的位移。

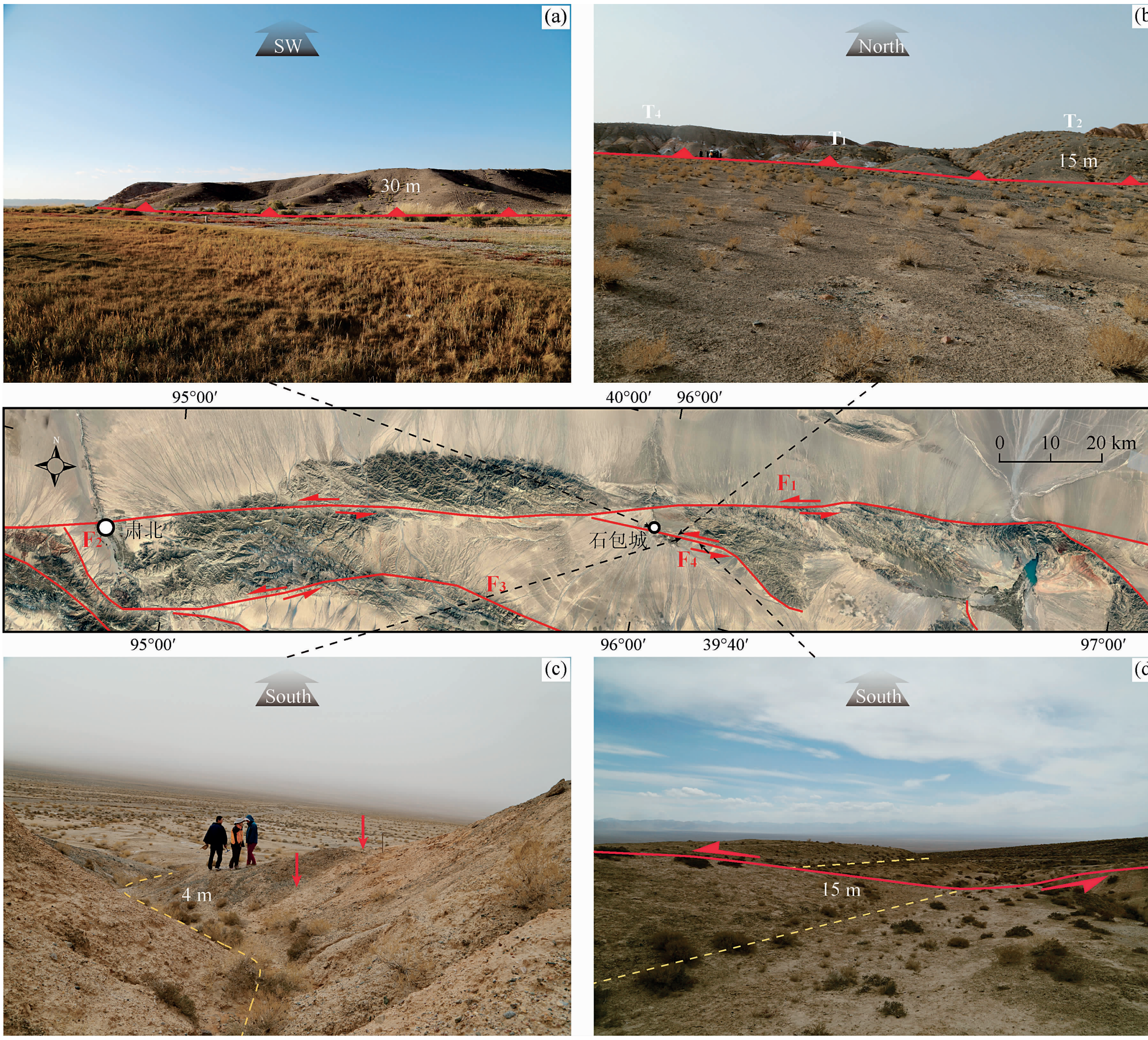

图 4　鹰嘴山南缘断裂构造地貌特征

Fig. 4　Structural geomorphic characteristics of South margin of Yingzui Mountain fault

(a)—断层陡坎;(b)—阶地断错地貌;(c)—冲沟左旋断错;(d)—阶地左旋断错;

F_1—阿尔北缘金断裂;F_2—党河南山断裂;F_3—野马河-大雪山断裂;F_4—鹰嘴山南缘断裂

(a)—Fault scarp in west segment of the South margin of Yingzui Mountain fault; (b)—offset terraces in west segment of the South margin of Yingzui Mountain fault; (c)—sinistral offset of the gully; (d)—sinistral offset of the terrace; F_1—North Altyn Tagh fault; F_2—Danghe South Mountain fault; F_3—Yema River-Daxue Mountain fault; F_4—South margin of Yingzui Mountain fault

2.3　疏勒河口—宽滩山段活动断裂发育特征

旱峡-大黄沟断裂与阿尔金断裂相交于疏勒河口东,全长 160 km,总体走向为北西西(图 2)。该断裂中新世—中更新世时段活动强烈,晚更新世以来处于相对稳定的状态。断裂的主要活动方式以挤压逆冲活动或者逆掩推覆活动为主,水平断错迹象不明显(图 5a)。近阿尔金断裂,主要表现为宽数十米的断层破碎带,其基岩断裂面产状为 235°∠70°,在山前发育的洪积扇山未发现明显的断错活动。因此我们推断旱峡-大黄沟断裂在晚更新世以来活动性减弱,不能大规模地吸收阿尔金断裂的左旋位移。然而,经过旱峡-大黄沟断裂以后阿尔金断裂的走向发生明显的变化,逆冲分量具有增大的趋势。Zhang Ning(2016)在该段选取 4 个点进行滑动速率的研究,近疏勒河口一带约为>1.58 mm/a,由西向东滑动速率逐渐减小。疏勒河口东 22 km 的滑动速率为 1.00~1.50 mm/a,红柳峡西疏勒河口东 32 km 为 0.58~0.72 mm/a。

但是野外调查发现现存断裂连续地表迹线东端可能位于地窝堡东,最新地表活动仍表现出明显的左旋滑动,冲沟的水平位移为 1.5~2 m,垂直位移约为 1 m,推测为同一次地震事件形成。孟家沙河与断裂的交汇处,河流的 T_1 阶地被左旋位移约 30 m,垂直位移量不大,因此认为在现存断裂地表迹线

的东端附近阿尔金断裂仍以左旋滑动为主。

在阿尔金断裂的南侧发育了一系列的次级分支断层和宽可达 8 km 的复背斜变形。这些次级分支断裂为复背斜前缘或者内部断裂。如赤金峡附近，在背斜的南翼，全新世活动明显，冲沟的各级阶地上分布一系列近似平行的陡坎(图 5d)，显示出明显的层间滑动的迹象。晚更新世砾石层发生明显的变形，南倾，倾角为 45°左右。复背斜东侧的赤金堡逆断层断续地分布在冲沟的 T_2 阶地上，与阿尔金断裂斜交。并未见到左旋的位移，最前缘断层的倾角约为 30°左右(图 5c)，上盘泥岩砂岩逆冲至全新世砾石层之上。通过野外测量和影像的解译对复背斜的产状进行统计分析，发现褶皱两翼的地层走向与阿尔金断裂的走向平行或小角度相交(图 5)，说明导致复背斜形成的挤压应力与阿尔金断裂走向垂直。该复背斜区可能是由于旱峡-大黄沟断裂北东向推挤，受到阿尔金断裂的阻挡的结果。因此沿阿尔金断裂南侧发育的复背斜没有大规模吸收阿尔金断裂左旋走滑的位移分量。在疏勒河口—宽滩山段除了赤金堡断裂，不存在其他活动性较强的次级断裂吸

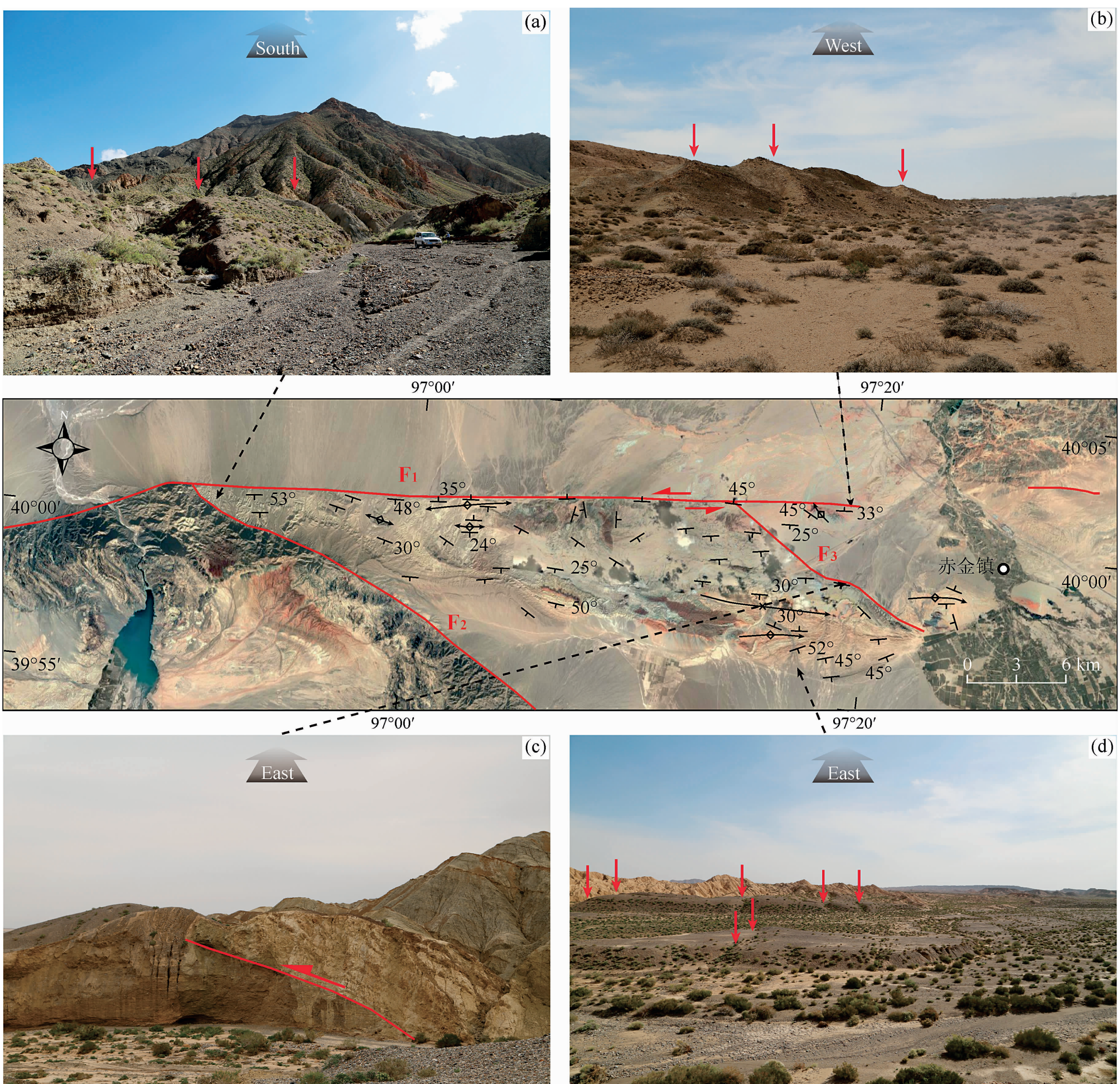

图 5 阿尔金断裂疏勒河以东段构造地貌特征

Fig. 5 Structural geomorphic characteristics of the east side area of Shule River mouth

(a)—旱峡-大黄沟断裂断错特征；(b)—阿尔金断裂东端的背斜；(c)—赤金断裂剖面；(d)—红柳峡背斜南缘；

F_1—阿尔北缘金断裂；F_2—旱峡-大黄沟断裂；F_3—赤金断裂

(a)—Offset characteristic of the Hanxia-Dahuanggou fault; (b)—fold in east end of the Altyn Tagh fault; (c)—profile of the Chijin fault;

(d)—south margin of the Hongliuxia fold; F_1—North Altyn Tagh fault; F_2—Hanxia-Dahuanggou fault; F_3—Chijin fault

收阿尔金断裂的左旋位移，该段的阿尔金断裂沿褶皱区左旋位移数量减小量不大，仍以非线性减小为主。

2.4　三联点构造演化模式

基于断裂三联点的展布特征我们推测党河南山断裂是青藏高原沿阿尔金断裂北东向挤出的派生断裂。党河南山断裂自形成初期至今可能经受了以下过程：在党河南山断裂形成初期可能与阿尔金断裂东段斜交(图 6a)，随着阿尔金断裂南侧物质的北东向挤出，党河南山断裂在拖曳作用下具有了左旋走滑的性质，此时野马河-大雪山断裂也可能开始了左旋的位移(图 6b)。青藏高原物质沿阿尔金断裂持续地向北东向推挤，党河南山断裂区呈叠瓦式逆冲断裂系(图 6c)。

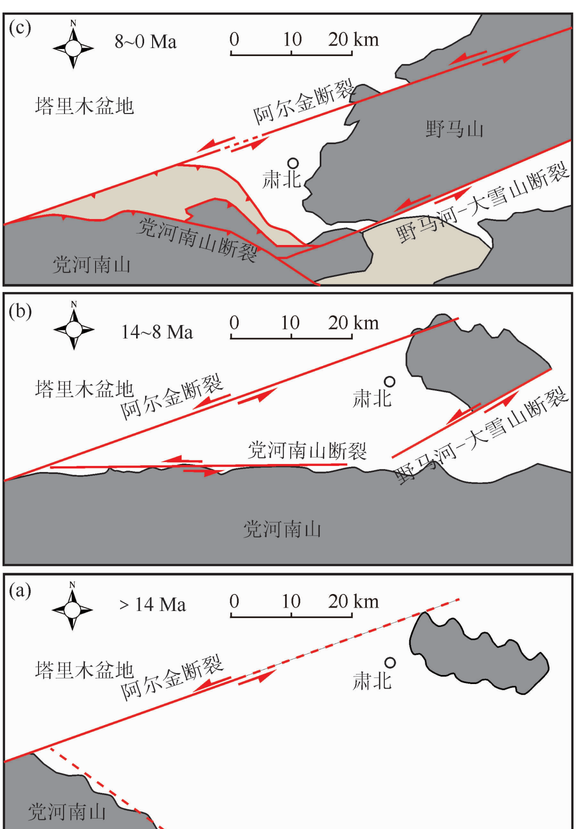

图 6　肃北三联点构造演化简图

Fig. 6　Schematic evolution map of Subei triple junction

(a)—>14 Ma 肃北三联点断裂分布特征；(b)—14～8 Ma 肃北三联点断裂分布特征；(c)—8～0 Ma 肃北三联点断裂分布特征

(a)—Spatial distribution of the faults in Subei triple junction before 14 Ma; (b)—spatial distribution of the faults in Subei triple junction during 14～8 Ma; (c)—spatial distribution of the faults in Subei triple junction during 8～0 Ma

与党河南山断裂系形成演化形式有所不同，鹰嘴山南缘断裂形成初期可能与阿尔金断裂东段斜交(图 7a)，随着青藏高原物质向北东向挤出，鹰嘴山沿着鹰嘴山南缘断裂向南仰冲，在其南侧与野马河-大雪山断裂共同形成了石包城盆地(图 7b)。高原物质的持续挤出，引起石包城盆地发生明显的顺时针旋转，新生了鹰嘴山南缘断裂近东西向段，鹰嘴山南缘断裂西段活动减弱，直至被废弃(图 7c)。

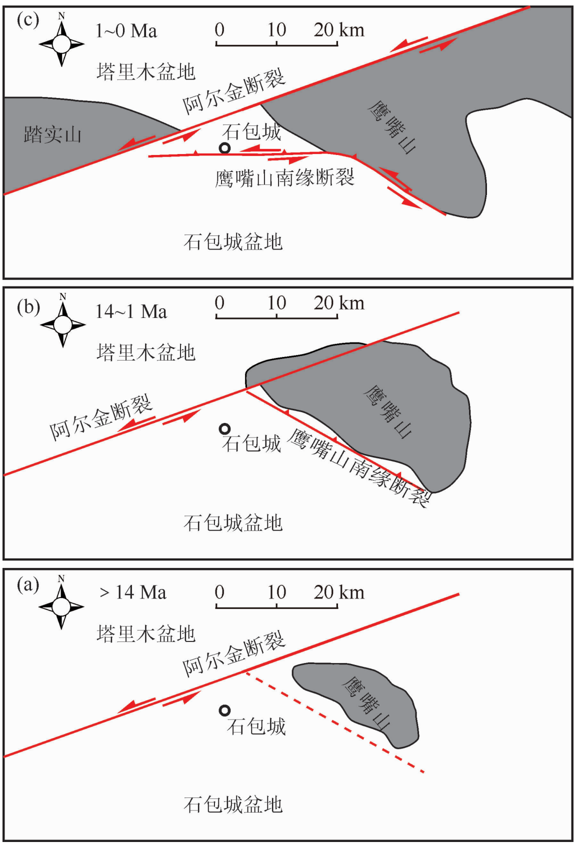

图 7　石包城三联点构造演化简图

Fig. 7　Schematic evolution map of Shibaocheng triple junction

(a)—>14 Ma 石包城三联点断裂分布特征；(b)—14～8 Ma 石包城三联点断裂分布特征；(c)—8～0 Ma 石包城三联点断裂分布特征

(a)—spatial distribution of the faults in Shibaocheng triple junction before 14 Ma; (b)—spatial distribution of the faults in Shibaochengi triple junction during 14～8 Ma; (c)—spatial distribution of the faults in Shibaocheng triple junction during 8～0 Ma

旱峡-大黄沟断裂在北祁连山形成初期与阿尔金断裂斜交(图 8a)，随后吸收了阿尔金断裂的左旋位移，导致了祁连山的迅速隆起(图 8b)。祁连山逆冲断裂带向北生长，受到了地块边界断裂阿尔金断裂的阻挡，不能继续向北扩展，随后在阿尔金断裂南侧形成红柳峡褶皱变形区(图 8c)，在褶皱区的西段主要是地层的单斜变形，部分靠近断裂的地层已经接近直立。此处主要发育了数组褶皱，阿尔金断裂主要沿着一组背斜的北翼延伸。红柳峡褶皱区吸收

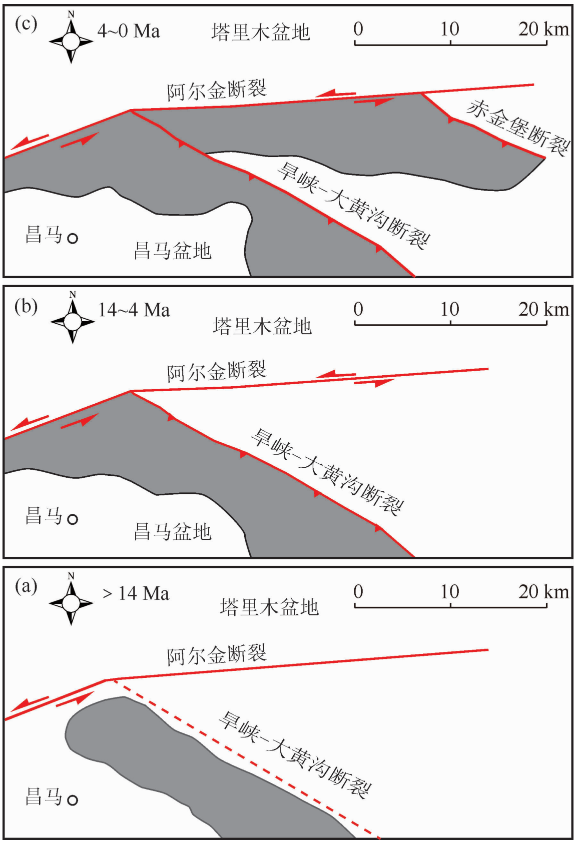

图 8 疏勒河口三联点构造演化简图

Fig. 8 Schematic evolution map of Shulehe triple junction

(a)—>14 Ma 疏勒河口三联点断裂分布特征;(b)—14～4 Ma 疏勒河口三联点断裂分布特征;(c)—4～0 Ma 疏勒河口三联点断裂分布特征

(a)—Spatial distribution of the faults in Shule River mouth triple junction before 14 Ma; (b)—spatial distribution of the faults in Shule River mouth triple junction during 14～4 Ma; (c)—spatial distribution of the faults in Shule River mouth triple junction during 4～0 Ma

了大量的近南北向的位移缩短,而且晚更新世以来极为活跃,旱峡-大黄沟断裂在晚更新世活跃性不强。可认为红柳峡褶皱区吸收了旱峡-大黄沟断裂的变形,导致了旱峡-大黄沟断裂吸收阿尔金断裂左旋位移的能力减弱。

基于三联点的变形模式,阿尔金断裂的左旋滑动位移被祁连山西段的逆冲断裂和走滑段所匹配。祁连山西段逆断裂引起的山脉的隆升与走滑断裂导致的构造转换与阿尔金断裂的北东向挤出呈明显的耦合关系。

3 阿尔金断裂东端点的确定

目前,关于阿尔金断裂滑动速率的研究结果存在争议,部分地质研究结果给出的滑动速率为大地测量学结果的 2～3 倍(图 9)。但是两个结果均显示在其东段阿尔金断裂的左旋滑动速率迅速减小。如前文所示,在地窝堡东侧(现存阿尔金断裂地表迹线东端),阿尔金断裂仍表现出明显的走滑现象,季节性河流的 T_1 阶地,山前的小型冲沟均显示出明显的左行位错。甚至在地表断裂地表痕迹消失的 500 m 处仍显示出明显的左旋活动,说明阿尔金断裂左旋位移活动到此并未终止。

阿尔金断裂沿宽滩山南缘向东穿过花海盆地与金塔南山断裂相连(Zheng Jiandong, 1991; Chen Wenbin and Xu Xiwei, 2006)。花海地区的物探剖面显示阿尔金断裂带的活动强度由西向东逐渐减弱(Xiao Qibin et al., 2011, 2015; Qin Suhua et al., 2013)。Zhang Bo et al. (2016)在金塔县西侧长山附近发现一系列的冲沟均被左旋断错,并选择两个典型的地貌点进行测量,估计金塔南山断裂的左旋走滑滑动速率约为 0.19 ± 0.05 mm/a。

金塔南山断裂及其东侧的断裂系在平面上构成向西收敛、向东撒开的斜列束状展布特征,这是典型的走滑断层尾端的几何结构(Chen Wenbin and Xu Xiwei, 2006),我们推测金塔南山断裂仍属于阿尔金断裂东端的延伸。在斜列束状展布断层最东端的桃花拉山-阿右旗断裂,以左旋走滑活动为主(Yu Jingxing et al., 2017)。Darby et al. (2005)基于北大山和合黎山的左旋断错位移,认为阿尔金断裂带早期至少延伸至北大山和合黎东侧,甚至可延伸至阿拉善右旗断裂(Tapponnier et al., 2001; Chen Wenbin and Xu Xiwei, 2006)。Zhang Jin et al. (2010)指出在 40～30 Ma 期间位于鄂尔多斯西侧的香山地区已经开始隆升并出现前陆盆地,说明欧亚板块的碰撞产生的应变当时已经影响到该地区,这为阿尔金断裂早期的侧向挤出提供了佐证。

经以上讨论,可认为阿尔金断裂层已延伸至阿拉善块体内部并形成明显的左旋位移。现今连续的地表破裂终止于玉门盆地西端,反映全新世以来阿尔金断裂东段活动性有所减弱(Luo Hao et al., 2019)。随着应变的累加,仍有可能引起金塔南山断裂与现今阿尔金断裂持续破裂带之间的全新世地表破裂空区再次贯通。

4 阿尔金断裂东段的演化模式

阿尔金断裂曾发生过多期活动,根据对阿尔金断裂带内同变形期新生矿物的激光微区 $^{39}Ar/^{40}Ar$ 测年结果,阿尔金断裂走滑活动有可能起始于 97～

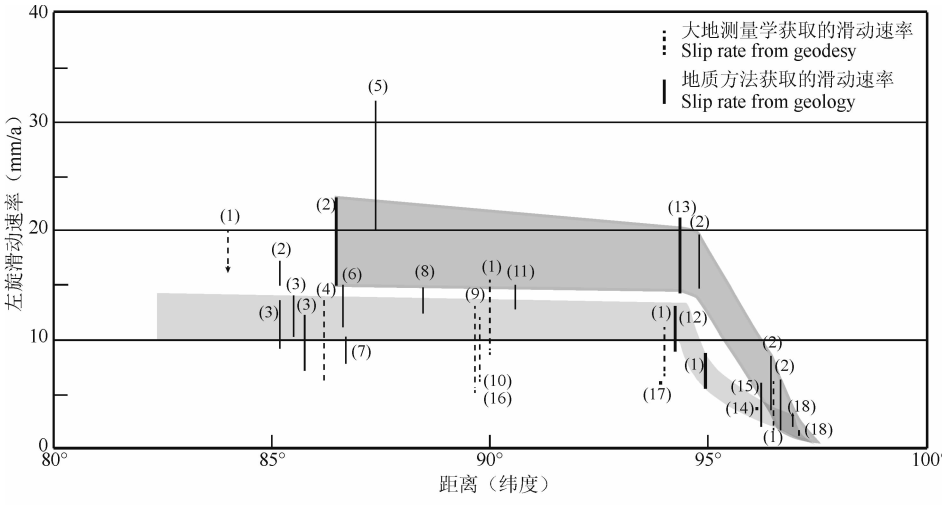

图 9　阿尔金断裂滑动速率分布图

Fig. 9　Slip rates along the Altyn Tagh fault

资料来源(Data from):(1) Zhang Peizhen et al., 2007;(2) Xu Xiwei et al., 2005;(3) Wang Feng 2002;(4) He Jiankun et al., 2013;(5) Mériaux et al., 2004;(6) Gold et al., 2011;(7) Gold et al., 2009;(8) Cowgill et al., 2009;(9) Bendick et al., 2000;(10) Wallace et al., 2004;(11) Mériaux et al., 2012;(12) Chen et al., 2013;(13) Mériaux et al., 2005;(14) Seong et al., 2011;(15) Meyer et al., 1998;(16) Yin Guanghua et al., 2002;(17) Xiang Hongfa et al., 2000;(18) Zhang Ning, 2016

89 Ma(Liu Yongjiang et al., 2000;Ge Xiaohong., 2001),这与 Kohistan 岛弧与欧亚板块的缝合时间 102～85 Ma 近于同步(Jin Zhenmin, 1999),暗示晚白垩纪以来由于 Kohistan 岛弧与欧亚板碰撞的远距离效应影响引起了阿尔金断裂的左旋走滑活动。

Darby et al.(2005)发现在白垩纪之后至中新世中前期,位于阿尔金断裂东端的北大山和合黎山至少发生了 70 km 的左旋位移,甚至引起断裂束总体 150 km 以上的左旋位移,说明在此时间段内阿尔金断裂曾发生大规模的左旋位移。Yuan Daoyang et al.(2013)同样认为 Kohistan 岛弧与与欧亚大陆碰撞初始,祁连山已经开始发生隆起(Cheng Xiaogan et al., 2016),但规模很小,无法对阿尔金断裂北东向侧向挤出造成显著的影响。

在 30 Ma 年左右,东昆仑造山带开始隆升(Mock et al., 1999; Joliet et al., 2001; Clark et al., 2010)。在至少 15 Ma 以前东昆仑断裂的西段开始形成张性盆地,并形成火山活动(Jolivet et al., 2003),表明此时东昆仑断裂开始发生大规模左旋位移。Duvall et al.(2013)指出东昆仑断裂近似的活动初始时间在 20～15 Ma 之间。

在中新世以来肃北地区古近纪左旋位移为 69～90 km(Wang Erchie, 1997),同时在大山和合黎山的左旋位移量＜5 km(Darby et al., 2005)。说明在中新世以后阿尔金断裂向北东方向的侧向挤出明显减弱。

15 Ma 以来,在青藏高原东北缘发生大规模的隆起,同时海原断裂开始形成(Duvall et al., 2013)。约 14 Ma 党河南山开始隆起(Lin Xu et al., 2015),这与我们在盐池湾背斜观测到的结果一致。10 Ma 左右北祁连山也开始大规模的隆起(Zheng Dewen et al., 2010; Wang Weitao et al., 2016)。Bedrosian et al.(2001)指出北山断裂和昌马断裂大约 5.5 Ma 以来水平缩短量分别为 14 km 和 7 km。而基于 Wang Erchie(1997)和 Darby et al.(2005)的研究结果可得到约 15 Ma 以来祁连山吸收了 65～85 km 的阿尔金断裂左旋位移。

因此我们认为在印度欧亚板块碰撞的初始,青藏高原的上地壳沿阿尔金断裂发生的侧向挤出,并未引起阿尔金断裂两侧大规模的隆起运动(图 10a)。此时,东昆仑和祁连山没有发生大规模的地壳缩短,仅吸收阿尔金断裂少量的左旋位移。由于岩石圈地幔迅速变薄(Turner et al., 1993),地块的薄弱带发生破坏。在 30 Ma 东昆仑地区发生大规模水平向的压缩变形、纵向的山脉隆起以及火山活动,随后的东昆仑断裂左旋位移开始大规模的吸收或转换阿尔金断裂的左旋位移。由于柴达木地区较为强硬,在东昆仑以北地区阿尔金断裂仍发生滑动速率近一致的侧向挤出活动(图 10b)。

在 15 Ma 以来祁连山脉加速隆起,缩短速率加

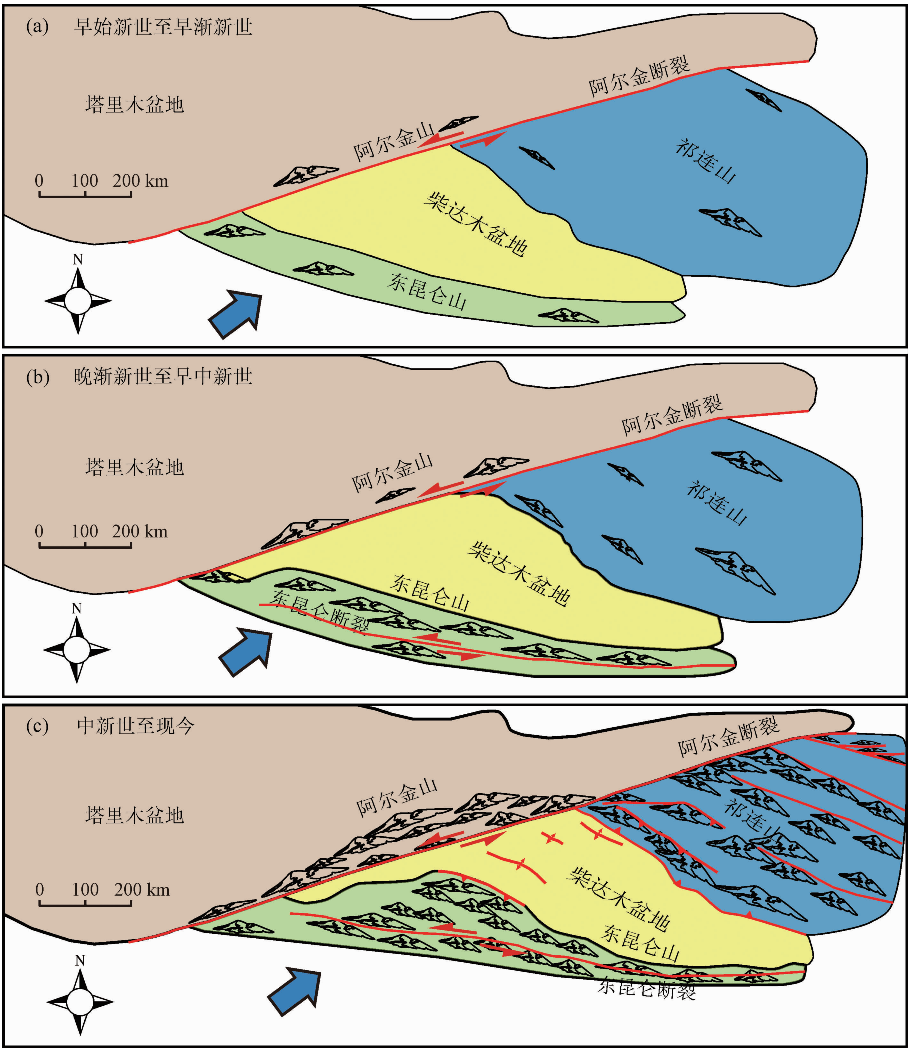

图 10 阿尔金断裂构造演化模式

Fig. 10 The sketch map of the growth of the North Qinghai-Tibet Plateau at the different times

(a)—早始新世至早渐新世，阿尔金断裂与山脉隆升的关系；(b)—晚渐新世至早中新世，阿尔金断裂与山脉隆升的关系；(c)—中新世至现今，阿尔金断裂与山脉隆升的关系

(a)—During the early Eocene to early Oligocene, relation between sinistral displacement of Altyn Tagh fault and uplifting of the mountain; (b)—during the late Oligocene to early Miocene, relation between sinistral displacement of Altyn Tagh fault and uplifting of the mountain; (c)—during the Miocene to today, relation between sinistral displacement of Altyn Tagh fault and uplifting of the mountain

快，几乎吸收了阿尔金断裂末端的全部左旋位移。因为软弱的地壳引起应变传播由侧向挤出转变为祁连山的隆升，导致祁连山地壳显著增厚(Li Hongyi et al., 2014)，以至阿尔金断裂不能有效地向外侧大规模的传递应力(图 10c)。

目前在柴达木盆地内部存在数量众多的背斜和逆断裂，压缩方向与阿尔金断裂的走向近似平行(Wei Yanyan et al., 2016)，目前柴达木地块正遭受破坏，发生 NEE 向的缩短。在盆地的东部，新构造活动更为强烈，鄂拉山和日月山在 10 Ma 左右迅速隆起(Yuan Daoyang et al., 2011)，在 NEE 向构造应力环境下开始右旋走滑活动(Yuan Daoyang et al., 2004)。因此可推测柴达木盆地可能正遭受由东向西逐渐闭合的活动。

5 结论

(1)阿尔金断裂的滑动速率在肃北—疏勒河口表现为非线性减小，祁连山西段的逆断裂和走滑断裂吸收了阿尔金断裂的左旋位移。在疏勒河口东，阿尔金断裂南侧发育的一系列褶皱变形并未大量吸收阿尔金断裂的左旋位移，滑动速率仍以非线性减小为主。

(2)阿尔金断裂连续破裂带现存迹线端点位于酒泉盆地西侧，其东侧的断裂束仍隶属于阿尔金断

裂,二者之间可能存在全新世地表破裂空区。

(3)自 Kohistan 岛弧与欧亚板块碰撞后,阿尔金断裂曾发生侧向挤出。随着东昆仑造山带和祁连山造山带的先后大规模隆起及其内部左旋走滑断层的形成,高原的侧向挤出能力迅速减弱。东昆仑造山带和祁连山造山带的活动性与阿尔金断裂北东向挤出能力存在明显的耦合关系。

致谢:非常感谢审稿专家对本文提出的宝贵意见和建议,让笔者获益良多。

References

Avouac J P, Tapponnier P. 1993. Kinematic model of active deformation in Central-Asia. Geophysical Research Letters, 20: 895～898.

Bedrosian P A, Unsworth M J, Wang F. 2001. Structure of the Altyn Tagh fault and Daxueshan from magnetotelluric surveys: implications for faulting associated with the rise of the Tibetan plateau. Tectonics, 20(4): 474～486.

Bendick R, Bilham R, Freymueller J, Larson K, Yin G. 2000. Geodetic evidence for a low slip rate in the Altyn Tagh fault system. Nature, 404(6773): 69～72.

Burchfiel B C, Deng Quidong, Molnar P, Royden L, Wang Yipeng, Zhang Peizhen, Zhang Weiqi. 1989. Intracrustal detachment within zones of continental deformation. Geology, 17(17): 748～752.

Chen Wenbin, Xu Xiwei. 2006. Sinistral strike-slip faults along the southern Alax margin and eastwards extendingof the Altyn Taghfault. Seismology and Geology, 28(2): 319～324 (in Chinese with English abstract).

Chen Yiwei, Li Shenghua, Sun Jimin, Fu Bihong. 2013. Osl dating of offset streams across the Altyn Tagh fault: channel deflection, loess deposition and implication for the slip rate. Tectonophysics, 594(3): 182～194.

Cheng Xiaogan, Lin Xiubin, Wu lei, Chen Hanlin, Xiao Anchen, Gong Junfeng, Zhang Fengqi, Yang, Shufeng. 2016. The exhumation history of north Qaidam thrust belt constrained by apatite fission track thermochronology: implication for the evolution of the Tibetan plateau. Acta Geologica Sinica (English Edition), 90(3): 870～883.

Clark M K, Farley K A, Zheng Dewen, Wang Zhicai, Duvall A R. 2010. Early Cenozoic faulting of the northern Tibetan plateau margin from apatite (U-Th)/He ages. Earth and Planetary Science Letters, 296(1～2): 78～88.

Cowgill E. 2001. Tectonic evolution of the Altyn Tagh-Western Kunlun fault system, northwestern China. Ph. D thesis of University of California.

Cowgill E. 2007. Impact of riser reconstructions on estimation of secular variation in rates of strike-slip faulting: revisiting the Cherchen River site along the Altyn Tagh fault, NW China, Earth and Planetary Science Letters, 254: 239～255.

Cowgill E, Gold R D, Chen Xuanhua, Wang Xiaofeng, Arrowsmith J R, Southon J. 2009. Low Quaternary slip rate reconciles geodetic and geologic rates along the Altyn Tagh fault, northwestern Tibet. Geology, 37(7): 647～650.

Cunningham D, Zhang Jin, Li Yanfeng. 2016. Late Cenozoic transpressional mountain building directly north of the Altyn Tagh fault in the Sanweishan and Nanjieshan, north Tibetan foreland, China. Tectonophysics, 687: 111～128.

Darby B J, Ritts B D, Yue Y J, Yue Yongjun, Men Qingren. 2005. Did the Altyn Tagh fault extend beyond the Tibetan plateau? Earth and Planetary Science Letters, 240: 425～435.

Delville N, Arnaud N, Montel J M, Roger F, Brunel M, Tapponnier P, Sobel E. 2001. Paleozoic to Cenozoic deformation along Altyn-Tagh fault in the Altun Shan massif area, eastern Qilian Shan, northeast Tibet, China. In: Hendrix M S, Davis G A, eds. Paleozoic and Mesozoic tectonic evolution of central and eastern Asia: from continental assembly to intracontinental deformation. Geological Society of America Memoir, 194: 269～292.

Duvall A R, Clark M K, Kirby E, Farley K A, Craddock W H, Li Chuanyou, Yuan Daoyang. 2013. Low-temperature thermochronometry along the Kunlun and Haiyuan faults, NE Tibetan plateau: evidence for kinematic change during late-stage orogenesis. Tectonics, 32: 1190～1211.

Ge Xiaohong, Liu Yongjiang, Ren Shoumai, Ye Huiwen, Pan Hongxun. 2001. Re-understanding on some academic problems of the Altun fault. Chinese Journal of Geology, 36(3): 319～325 (in Chinese with English abstract).

Gold R D, Cowgill E, Arrowsmith J R, Chen X, Sharp W D, Cooper K M, Wang Xiaofeng. 2011. Faulted terrace risers place new constraints on the late Quaternary slip rate for the central Altyn Tagh fault, northwest Tibet. Geological Society of America Bulletin, 123(5～6): 958～978.

Gold R D, Cowgill E, Arrowsmith J R, Gosse J, Chen Xiangming, Wang Xiaofeng. 2009. Riser diachroneity, lateral erosion, and uncertainty in rates of strike-slip faulting: a case study from Tuzidun along the Altyn Tagh fault, NW China. Journal of Geophysical Research, 114(B4), 377～381.

Hanson A D. 1999, Organic geochemistry and petroleum geology, tectonics and basin analysis of southern Tarim and northern Qaidam Basins, northwest China. Ph. D thesis of Stanford University, 1～388.

He Jiankun, Philippe V, Jean C, Wang Weimin, Lu Shuangjiang, Ku Wenfei, Xia Wenhai, Bilham R. 2013. Nailing down the slip rate of the Altyn Tagh fault. Geophysical Research Letters, 40(20): 5382～5386.

Jin Zhenmin. 1999. Discovery of coesite-bearing eclogite from west Himalyan tectonic link and its enlightenment. Geological Science and Technology Information, 18(3): 1～5 (in Chinese with English abstract).

Jolivet M, Brunel M, Seward D, Xu Zhenbo, Yang J, Roger F, Tapponnier P, Malavieille J, Arnaud N, Wu C. 2001. Mesozoic and cenozoic tectonics of the northern edge of the tibetan plateau: fission-track constraints. Tectonophysics, 343(1～2): 111～134.

Jolivet M, Brunel M, Seward D, Xu Z, Yang J, Malavieille J, Roger F, Leyreloup A, Arnaud N, Wu C. 2003. Neogene extension and volcanism in the Kunlun fault zone, northern Tibet: new constraints on the age of the Kunlun fault. Tectonics, 22(5): 1～23.

Kirby E, Harkins N, Wang Eeqi, Shi Xuhua, Fan Chun, Burbank D. 2007. Slip rate gradients along the eastern Kunlun fault. Tectonics, 26: 485～493.

Li Hongyi, Yang Shen, Huang Zhongxian, Li Xinfu, Gong Meng, Shi Dannian, Sandvol E, Li Aibing. 2014. The distribution of the mid-to-lower crustal low-velocity zone beneath the northeastern Tibetan plateau revealed from ambient noise tomography. Journal of Geophysical Research: Solid Earth, 119(3): 1954～970.

Li Haibing, Yang Jingsui Xu Zhiqin, Wu Cailai, Zhang Jianxin, Wan Yusheng, Shi Rendeng, Liou J G, Ireland T R. 2000. Age of the Altyn Tagh strike-slip fault. Beijing, China University of Geosciences, 15th Himalaya-Karakoram-Tibet Workshop Abstract Volume, 1～208.

Li Yuhang, Wang Qinglian, Cui Duxin, Hao Ming, Wang Wenping, Qin Shanlan. 2015. Inversion of present-day fault slip rate along Altyn Tagh fault constrained by GPS date. Seismology and Geology, 37(3): 869～879 (in Chinese with English abstract).

Lin Xu, Zheng Dewen, Sun Jimin, Windley B F, Tian Zhonghua, Gong Zhijun, Jia Yingying. 2015. Detrital apatite fission track evidence for provenance change in the Subei Basin and implications for the tectonic uplift of the Danghe Nan Shan (NW China) since the mid-Miocene. Journal of Asian Earth Sciences, 111: 302～311.

Liu Yongjiang, Ye Huiwen, Ge Xiaohong, Chen Wen, Liu Junlai, Ren Shoumai, Pan Hongxun. 2000. Laser probe $^{40}Ar/^{39}Ar$ dating of micas on the deformed rocks from Altyn fault and its tectonic implications. Chinese Science Bulletin, 45(19): 2101～2104 (in Chinese with English abstract).

Lu Haijian, Fu Bihong, Shi Pilong, Ma Yuanxu, Li Haibing. 2016. Constraints on the uplift mechanism of northern Tibet. Earth and Planetary Science Letters, 453: 108～118.

Luo Hao, He Wengui, Wang Dingwei, Yuan Daoyang, Shao Yanxiu. 2013a. Study on the slip rate on Changma fault in Qilian Mountains since Late Pleistocene. Seismology and Geology. 35(4): 765～777 (in Chinese with English abstract).

Luo Hao, He Wengui, Yuan Daoyang, Shao Yanxiu. 2013b. The Holocene activity evidences of Yema River-Daxue Mountain fault in western Qilian Mountain. Acta Geologica Sinica (English Edition), 87(6): 1569～1584.

Luo Hao, He Wengui, Yuan Daoyang, Shao Yanxiu. 2015. Slip rate of Yema River-Daxue mountain fault since the Late Pleistocene and its implications on the deformation of the northeastern margin of the Tibetan plateau. Acta Geologica Sinica (English Edition), 89(2): 561～574.

Luo Hao, Xu Xiwei, Gao Zhanwu, Liu Xiaoli, Yu Hongmei, Wu Xiyan. 2019. Spatial and temporal distribution of earthquake ruptures in the eastern segment of the Altyn Tagh fault, China. Journal of Asian Earth Sciences, 173: 263～274.

Mériaux A S, Ryerson F J, Tapponnier P, van der Woerd J, Finkel R C, Xu Xiwei, Xu Zhiqin, Caffe M W. 2004. Rapid slip along the central Altyn Tagh fault: morphochronoleogic evidence from Cherchen He and Sulamu Tagh. Journal of Geophysical Research: Atmospheres, 109(B6): 611～616.

Mériaux A S, Tapponnier P, Ryerson F J, Xu Xiwei, King G, Van der Woerd J, Finkel R C, Li Haibing, Xu Zhiqin, Chen Wenbin. 2005. The Aksay segment of the northern Altyn Tagh fault: tectonic geomorphology, landscape evolution, and Holocene slip rate. Journal of Geophysical Research: Atmospheres, 110(B4): 229～246.

Mériaux A S, van der Woerd J, Tapponnier P, Ryerson F J, Finkel R C, Lasserre C, Xu Xiwei. 2012. The pingding segment of the Altyn Tagh fault (91E): Holocene slip-rate determination from cosmogenic radionuclide dating of offset fluvial terraces. Journal of Geophysical Research: Solid Earth, 117(B9): 469～478.

Métivier F, Gaudemer Y, Tapponnier P, Meyer B. 1998. Northeastward growth of the Tibet plateau deduced from balanced reconstruction of two depositional areas: the Qaidam and Hexi Corridor basins, China. Tectonics, 17: 823～842.

Meyer B, Tapponnier P, Bourjot L, Metivier F, Gaudemer Y, Peltzer G, Guo Shunmin, Chen Zhitai. 1998. Crustal thickening in Gansu-Qinghai, lithospheric mantle subduction, and oblique, strike-slip controlled growth of the Tibet plateau. Geophysical Journal International, 135: 1～47.

Meyer B, Tapponnier P, Gaudemer Y, Peltzer G, Guo Shunmin, Chen Zhitai. 1996. Rate of left-lateral movement along the easternmost segment of the Altyn Tagh fault, east of 96E (China). Geophysical Journal International, 124(124): 29～44.

Mock C, Arnaud N O, Cantagrel J M. 1999. An early unroofing in northeastern Tibet? Constraints from $^{40}Ar/^{39}Ar$ thermochronology on granitoids from the eastern kunlun range (Qianghai, NW China). Earth and Planetary Science Letters, 171(1): 107～122.

Molnar P, Caent L. 1989. Fault plane solutions of earthquakes and active tectonics of the Tibetan plateau and its margins. Geophysical Journal International, 99: 123～154.

Molnar P, Stock J M. 2009. Slowing of India's convergence with Eurasia since 20 Ma and its implications for Tibetan mantle dynamics. Tectonics, 28, No. TC3001, doi: 10.1029/ 2008TC002271.

Molnar P, Tapponnier P. 1978. Active tectonics of Tibet. Journal of Geophysical Research: Atmospheres, 83: 5361～5376.

Peltzer G, Armijo R. 1989. Magnitude of late Quaternary left-lateral displacements along the north edge of Tibet. Science, 246: 1285～1289.

Peltzer G, Tapponnier P. 1988. Formation and evolution of strike-slip faults, rifts, and basins during the India-Asia Collision: An experimental approach. Journal of Geophysical Research: Atmospheres, 93: 15085～15117.

Qin Suhua, Wang Xiaoshan, Kang Nanchang, He Baowei, Bai Jun, Pang Xueyan, Duan Xinhong, Wu Zhankui. 2013. An analysis of the effect from Altyn fault upon Jiuquan basin. Acta Petrologica Sincia, 29(8): 2895～2905 (in Chinese with English abstract).

Qiu Aimei, Li Baixiang. 2011. A tentative discussion on the tail effect on northeast Altun fault belt in the light of geophysical field information. Geophysics and Geochemical Exploration, 35(2): 149～154 (in Chinese with English abstract).

Seong Y B, Kang H C, Ree J H, Yi C, Yoon H. 2011. Constant slip rate during the late Quaternary along the Sulu He segment of the Altyn Tagh fault near Changma, Gansu, China. Island Arc, 20(1): 94～106.

Shao Yanxiu, Yuan Daoyang, Lei Zhongsheng, Liu Xingwang, Luo Hao. 2011. The features of earthquake surface rupture zone on northern margin fault of Danghe Nanshan. Technology for Earthquake Disaster Prevention, 6(4): 427～435 (in Chinese with English abstract).

Sun Jimin, Zhu Rixiang, An Zhisheng. 2005. Tectonic uplift in the northern Tibetan plateau since 13.7 Ma ago inferred from molasse deposits along the Altyn Tagh fault. Earth and Planetary Science Letters 235: 641～653.

Tapponnier P, Xu Zhiqin, Roger F, Meyer B, Arnaud N, Wittlinger G, Yang Jingsui. 2001. Oblique stepwise rise and growth of the Tibet plateau. Science, 294: 1671～1677.

Turner S, Hawkesworth C, Liu J, Rogers N, Kelley S, van Calsteren P. 1993. Timing of Tibetan uplift constrained by analysis of volcanic rocks. Nature, 364(6432): 50～54.

Van der Woerd J, Ryerson F J, Tapponnier P, Gaudemer Y, Finkel R, Meriaux A S, Caffee M, Zhao G, He Q. 1998. Holocene left-slip rate determined by cosmogenic surface dating on the Xidatan segment of the Kunlun fault (Qinghai, China). Geology, 26(8): 695～698.

Van der Woerd J, Ryerson F J, Tapponnier P, Mériaux A S, Gaudemer Y, Meyer B, Finkel R C, Caffee M W, Zhao G, Xu Zhiqin. 2000. Uniform slip-rate along the Kunlun fault: implication for seimic behaviour, large-scale tectonics and climatic imprint on Tibetan landforms. Geophysical Research Letters, 27(16): 2353～2356.

Van der Woerd J, Xu Xiwei, Li Haibing, Tapponnier P, Meyer B, Ryerson F J, Meriaux A S, Xu Zhiqin. 2001. Rapid active thrusting along the northwestern range front of the Tanghe Nan Shan (western Gansu, China). Journal of Geophysical Research: Solid Earth, 106(B12): 1～30.

Wallace K, Yin G, Bilham R. 2004. Inescapable slow slip on the Altyn Tagh fault. Geophysical Research Letters, 31(9): 399～420.

Wang Erchie. 1997. Displacement and timing along the northern strand of Altyn Tagh fault zone, northern Tibet. Earth and Planetary Science Letters, 150: 55～64.

Wang Feng. 2002. Slip-rates and segmentation feature of surface ruptures caused by earthquakes along the Altyn Tagh fault zone sincelate Quaternary. Institute of Geology, China Earthquake Administration, 1～86 (in Chinese with English abstract).

Wang Weitao, Zhang Peizhen, Pang Jianzhang, Garzione C, Zhang Huiping, Liu Caicai, Zheng Dewen, Zheng Wenjun, Yu Jixing. 2016. The Cenozoic growth of the Qilian Shan in the northeastern Tibetan plateau: a sedimentary archive from the Jiuxi basin. Journal of Geophysical Research: Solid Earth, 121

(4): 2235～2257.

Wei Yanyan, Xiao Ancheng, Wu Lei, Mao Liguang, Zhao Haifeng, Shen Ya, Wang Liqun. 2016. Temporal and spatial patterns of Cenozoic deformation across the Qaidam Basin, northern Tibetan plateau. Terra Nova, 28: 409～418.

Wittlinger G, Tapponnier P, Poupinet G, Mei J, Shi D, Herquel G, Masson F. 1998. Tomographic evidence for localized lithospheric shear along the Altyn Tagh fault. Science, 282: 74～76.

Wu Lei, Gong Qinglin, Qin Suhua. 2013. When did Cenozoic left-slip along the Altyn Tagh fault initiate? A conprehensive approach. Acta Petrologica Sinca, 29(8): 2837～2850 (in Chinese with English abstract).

Wu Lei, Xiao Ancheng, Wang Liqun, Mao Liguang, Wang Liang, Dong Youpu, Xu Bo. 2012a. EW-trending uplifts along the southern side of the central segment of the Altyn Tagh fault, NW China: insight into the rising mechanism of the Altyn Mountain during the Cenozoic. Science China: Earth Sciences, 55: 926～939.

Wu Lei, Xiao Ancheng, Yang Shufeng, Wang Liqun, Mao Ligang, Wang Liang, Dong Youpu, Xu Bo. 2012b. Two-stage evolution of the Altyn Tagh fault during the Cenozoic: New insight from provenance analysis of a geological section in NW Qaidam basin, NW China. Terra Nova, 24(5): 387～395.

Xiang Hongfa, Guo Shunmin, Zhang Wanxia, Zhang Bingliang. 2000. River offset and slip rate of the east segment of Altyn Tagh fault zone since Quaternary. Seimology and Geology, 22(2): 129～138 (in Chinese with English abstract).

Xiao Qibin, Shao Guihang, Liu Zengjing, Oskin M E, Zhang Jin, Zhao Guoze, Wang Jijun. 2015. Eastern termination of the Altyn Tagh fault, western China: constraints from a magnetotelluric survey. Journal of Geophysical Research: Solid Earth, 27(4): 609～614.

Xiao Qibin, Zhao Guoze, Dong Zeyi. 2011. Electrical resistivity structure at the northern margin of the Tibetan plateau and tectonic implications. Journal of Geophysical Research: Solid Earth, 116(B12): 7926～7926.

Xu Xiwei, Wang Feng, Zheng Rongzhang, Chen Wenbin, Ma Wentao, Yu Guihua, Chen Guihua, Tapponnier P, van Der Woerd J, Meriaux A. 2005. Late Quaternary sinistral slip rate along the Altyn Tagh fault and its structural transformation model. Science in China Series D: Earth Sciences, 48: 384～397.

Yin An, Kapp P A, Murphy M A, Manning C E, Harrison T M, Grove M, Ding Lin, Deng Xiguang, Wu Cunming. 1999. Significant late Neogene east-west extension in northern Tibet. Geology, 27: 787～790.

Yin An, Rumelhart P E, Butler R, Cowgill E, Harrison T M, Foster D A, Ingersoll R V, Zhang Qing, Zhou Xianqiang, Wang Xiaofeng, Hanson A, Raza A. 2002. Tectonic history of the Altyn Tagh fault system in northern Tibet inferred from Cenozoic sedimentation. Geological Society of America Bulletin, 114: 1257～1295.

Yin Guanghua, Jiang Jingxiang, Zhu Lingren, Bilham, R Bendick R. 2002. Present～day motion velocity of Wuzhunxiao segment of Altyn Tagh fault. Journal of Geodesy and Geodynamics, 22(3): 52～55 (in Chinese with English abstract).

Yu Hongmei, Xu Jiandong, Zhao Bo, Shen Huanhuan, Lin Chuanyong. 2014. Magmatic process of Ashi volcano, western Kunlun Mountains, China. Acta Geologica Sinica (English Edition), 88(2): 530～543.

Yu Jingxing, Zheng Wenjun, Kirby E, Zhang Peizhen, Lei Qiyun, Ge Weipeng, Wang Weitao, Li Xinnan, Zhang Ning. 2016. Kinematics of late Quaternary slip along the Yabrai fault: Implications for cenozoic tectonics across the Gobi Alashan block, China. Lithosphere, 8(3): 199～218.

Yu Jingxing, Zheng Wenjun, Lei Qiyun, Shao Yanxiu, Ge Weipeng, Ma Yan, Li Wenjuan. 2013. Neotectonics and kinematics along the Yabrai range-front fault in the south Alaxblock and its implications for regional tectonics. Seismology and Geology, 35(4): 731～744 (in Chinese with English abstract).

Yu Jingxing, Zheng Wenjun, Zhang Peizhen, Lei Qiyun, Wang Xulong, Wang Weitao, Li Xinan, Zhang Ning. 2017. Late Quaternary strike-slip along the Taohuala Shan-Ayouqi fault zone and its tectonic implications in the Hexi Corridor and the southern Gobi Alashan, China. Tectonophysics, 721: 28～44.

Yuan Daoyang, Champagnac J D, Ge Weipeng, Molnar P, Zhang Peizhen, Zheng Wenjun, Zhang Huipin, Liu Xingwang. 2011. Late Quaternary right-lateral slip rates of faults adjacent to the lake Qinghai, northeastern margin of the Tibetan plateau. Geological Society of America Bulletin, 123(9～10), 2016～2030.

Yuan Daoyang, Ge Weipeng, Chen Zhengwei, Li Chuanyou, Wang Zhicai, Zhang Huiping, Zhang Peizhen, Zheng Dewen, Zheng Wenjun, Craddock W H, Dayem K E, Duvall A R, Hough B G, Lease R O, Champagnac J-D, Burbank D W, Clark M K, Farley K A, Garzione C N, Kirby E, Molnar P, Roe G H. 2013. The growth of northeastern Tibet and its relevance to large-scale continental geodynamics: a review of recent studies. Tectonics, 32(5): 1358～1370.

Yue Yongjun, Bradley D R, Graham S A. 2001. Initiation and long-term slip history of the Altyn Tagh fault. International Geology Review, 43: 1087～1093.

Yue Yongjun, Liou J G. 1999. Two-stage evolution model for the Altyn Tagh fault, China. Geology, 27(3): 227～230.

Yun Long, Zhang Jin, Xiao Qibin, Wang Ju, Ling Hui, Luo Hui, Tian Xiao, Zhang Jingjia. 2019. Thrust movement and deep structural characteristic of the Sanweishan fault in the northern margion of the Tibetanplateau since the late Quaternary. Acta Geologica Sinica, 93(9): 2017～2122 (in Chinese with English abstract).

Zhang Bo, He Wengui, Pang Wei, Wu Zhao, Shao Yanxiu, Yuan Daoyang. 2016. Geological and geomorphic expressions of late Quaternary strike-slip activity on Jinta Nanshan fault in northern edge of Qing-Zang block. Seismology and Geology, 38(1): 1～21 (in Chinese with English abstract).

Zhang Jin, Cunningham Dickson, Cheng Hongyi. 2010. Sedimentary characteristics of Cenozoic strata in central-southern Ningxia, NW China: implications for the evolution of the NE Qinghai-Tibetan Plateau. Journal of Asian Earth Sciences, 39: 740～759.

Zhang Ning. 2016. Geometry and kinematics of the eastern end of the Altyn Tagh fault. Institute of Geology, CEA: 1～75.

Zhang Peizhen, Molnar P, Xu Xiwei. 2007. Late Quaternary and present-day rates of slip along the Altyn Tagh fault, northern margin of the Tibetan plateau. Tectonics, 26: doi: 10.1029/2006 TC002014.

Zhang Yongshuang, Yao Xin, Du Guoliang, Guo Changbao. 2016. Late-quaternary slip rate and seismic activity of the Xianshuihe fault zone in southwest China. Acta Geologica Sinica (English Edition), 90(2): 525～536.

Zhang Yueqiao, Li Hailong, Li Jian. 2016. Neotectonics of the eastern margin of the Tibetan plateau: new geological evidence for the change from early pleistocene transpression to late Pleistocene-Holocene strike-slip faulting. Acta Geologica Sinica (English Edition), 90(2): 467～485.

Zheng Dewen, Clark M K, Zhang Peizhen, Zheng Wenjun, Farley K A. 2010. Erosion, fault initiation and topographic growth of the North Qilian Shan (northern Tibetan plateau). Geosphere, 6:937～941.

Zheng Jiandong. 1991. Geometry of the Altun fracture zone. Regional Geology of China, (1): 54～59 (in Chinese with English abstract).

Zheng Wenjun, Zhang Peizhen, He Wengui, Yuan Daoyang, Shao Yanxiu, Zheng Dewen, Ge Weipeng, Min Wei. 2013a. Transformation of displacement between strike-slip and crustal shortening in the northern margin of the Tibetan plateau:

evidence from decadal GPS measurements and late Quaternary slip rates on faults. Tectonophysics, 584: 267～280.
Zheng Wenjun, Zhang Huiping, Zhang Peizhen, Molnar P, Liu Xingwang, Yuan Daoyang. 2013b. Late quaternary slip rates of the thrust faults in western Hexi corridor (northern Qilian Shan, China) and their implications for northeastward growth of the Tibetan plateau. Geosphere, 9(2): 342～354.

参 考 文 献

陈文彬，徐锡伟. 2006. 阿拉善地块南缘的左旋走滑断裂与阿尔金断裂带的东延. 地震地质，28(2)：319～324.
葛肖虹，刘永江，任收麦，叶慧文，刘俊来，潘宏勋. 2001. 对阿尔金断裂科学问题的再认识. 地质科学，36(3)：319～325.
国家地震局《阿尔金滑动断裂带》课题组. 1992. 阿尔金活动断裂带. 北京：地震出版社.
金振民. 1999. 喜马拉雅造山带西构造结含柯石英榴辉岩的发现及其启示. 地质科技情报，18(3)：1～5.
李煜航，王庆良，崔笃信，郝明，王文萍，秦姗兰. 2015. 利用GPS数据反演阿尔金断裂现今滑动速率. 地震地质，37(3)：869～879.
刘永江，叶慧文，葛肖虹，陈文，刘俊来，任收麦，潘洪勋. 2000. 阿尔金断裂变形岩激光微区龄^{39}Ar/^{40}Ar 及其构造意义. 科学通报，45(19)：2101～2104.
罗浩，何文贵，王定伟，袁道阳，邵延秀. 2013. 祁连山昌马断裂晚更新世滑动速率. 地震地质，35(4)：765～777.
覃素华，王小善，康南昌，贺保卫，白军，庞雪燕，段新红，吴占奎. 2013. 阿尔金断裂对酒泉盆地的控制作用分析. 岩石学报，29(8)：2895～2905.
邱爱美，李百祥. 2011. 从地球物理场信息探讨阿尔金断裂带东北尾端效应和延伸. 物探与化探，35(2)：149～154.
邵延秀，袁道阳，雷中生，刘兴旺，罗浩. 2011. 党河南山北缘断裂古地震形变带特征研究. 震灾防御技术，6(4)：427～435.
王峰. 2002. 阿尔金断裂带晚第四纪滑动速率及其地震地表破裂分段特征. 中国地震局地质研究所，1～86.
吴磊，巩庆霖，覃素华. 2013. 阿尔金断裂新生代大规模走滑起始时间的厘定. 岩石学报，29(8)：2837～2850.
向宏发，虢顺民，张晚霞，张秉良. 2000. 阿尔金断裂带东段第四纪以来水系位错与滑动速率. 地震地质，22(2)：129～138.
尹光华，蒋靖祥，朱令人，Bilham R, Bendick R. 2002. 阿尔金断裂乌尊硝段的现今活动速率. 大地测量与地球动力学，22(3)：52～55.
俞晶星，郑文俊，雷启云，邵延秀，葛伟鹏，马严，李又娟. 2013. 阿拉善地块南部雅布赖山前断裂的运动学特征及意义初探. 地震地质，35(4)：731～744.
袁道阳，张培震，刘百篪，甘卫军，毛凤英，王志才，郑文俊，郭华. 2004. 青藏高原东北缘晚第四纪活动构造的几何图像与构造转换. 地质学报，78(2)：270～278.
云龙，张进，肖骑斌，王驹，凌辉，罗辉，田宵，张竞嘉. 2019. 青藏高原北缘三危山断裂晚第四纪以来的逆冲运动及其深部构造特征. 地质学报，93(9)：2017～2122.
张波，何文贵，庞炜，吴赵，邵延秀，袁道阳. 2016. 青藏块体北部金塔南山断裂晚第四纪走滑活动的地质地貌特征. 地震地质，38(1)：1～21.
张宁. 2016. 阿尔金断裂东端部的几何结构与运动特征. 中国地震局地质研究所，1～75.
郑剑东. 1991. 阿尔金断裂带的几何学研究. 中国区域地质，(1)：54～59.

The structural deformation pattern in the eastern segment of the Altyn Tagh fault

LUO Hao*[1)], XU Xiwei[2)], LIU Xiaoli[3)], BAI Luanxi[4)], WANG Qixin[4)], LI Mengni[4)], LIU Shaozhuo[4)]
1) *China Earthquake Disaster Prevention Center, China Earthquake Administration, Beijing*, 100029;
2) *Institute of Crustal Dynamics, China Earthquake Administration, Beijing*, 100085;
3) *Key Laboratory of Earthquake Geodesy, Institute of Seismology, China Earthquake Administration, Wuhan*, 430071;
4) *Key Laboratory of Active Tectonics and Volcano, Institute of Geology, China Earthquake Administration, Beijing*, 100029
* *Corresponding author: hy-luo@163.com*

Abstract

The large left lateral strike-slip faults are responsible for the continental deformation of the Qinghai-Tibet Plateau. Recent studies on the Altyn Tagh fault have called attention to the growth of the northern edge of the Plateau. Field survey and previous results suggest that the slip rate of the Altyn Tagh fault abruptly decreased on two sides of the triple junction from the Subei County to the Shule River. The thrust faults, strike faults in the western segment of the Qilian Mountain have absorbed the sinistral displacement of the Altyn Tagh fault, and thus the present trace disappeared in west of Jiuquan basin. But the Altyn Tagh fault had extended into the Alxa block before mid-Miocene. The Plateau began to extend laterally along the Altyn Tagh fault at the almost same slip rate after collision between the Kohistan and Eurasian plates, and there is no obvious uplift on both sides of the fault. Then, the East Kunlun and Qilian orogenic belts prominently uplifted successively, and the lateral extension of the Altyn Tagh fault rapidly decreased. Therefore, a coupling interaction exists between the extrusion of the Altyn Tagh fault and the uplift of the East Kunlun and Qilian orogenic belts.

Key words: strike-slip fault; transform model; Altyn Tagh fault; Qilian Mountain; Qinghai-Tibet Plateau